



Passive and Active Control on 3D Convective Flow of Viscoelastic Nanofluid With Heat Generation and Convective Heating

S. Eswaramoorthi¹ and M. Bhuvaneshwari^{2*}

¹ Department of Mathematics, Dr. N.G.P. Arts and Science College, Coimbatore, India, ² Department of Mathematics, Kongunadu Polytechnic College, Dindigul, India

The present article addresses the impact of passive control (PC) and active control (AC) on 3D flow of a viscoelastic nanofluid upon a stretching plate including heat generation and convective heating. The system of appearing non-linear PDE's are converted into a couple of ODE's by using suitable similarity transformations. Convergent series solutions are derived using the homotopy analysis method (HAM). Graphical results of velocity, nanoparticle volume fraction and temperature of different pertinent physical parameters with notable discussions are mentioned along with their physical significance.

OPEN ACCESS

Edited by:

Dipankar Chatterjee,
Central Mechanical Engineering
Research Institute (CSIR), India

Reviewed by:

Sankar M,
Presidency University, India
Suvankar Ganguly,
Tata Steel, India

*Correspondence:

M. Bhuvaneshwari
msubhvana@yahoo.com

Specialty section:

This article was submitted to
Thermal and Mass Transport,
a section of the journal
Frontiers in Mechanical Engineering

Received: 04 October 2018

Accepted: 31 May 2019

Published: 20 June 2019

Citation:

Eswaramoorthi S and
Bhuvaneshwari M (2019) Passive and
Active Control on 3D Convective Flow
of Viscoelastic Nanofluid With Heat
Generation and Convective Heating.
Front. Mech. Eng. 5:36.
doi: 10.3389/fmech.2019.00036

Keywords: viscoelastic nanofluid, heat generation, passive/active control, convective heating, convection, stretching plate, HAM

1. INTRODUCTION

Fluids are much used to transfer heat in heat transfer equipment in industrial and engineering processes. Such processes are die casting, catalysis, distillation, synthesis in petrochemical industry, gas processing, hot-mix paving in concrete industry and steam generators in industrial laundry. In the above applications, thermal conductivity plays a vital role in heat transfer equipment. Conventional heat transfer of ordinary fluids, like water and oil, have low thermal conductivity, and poor heat transfer characters. The nanofluid is an advanced type of fluid incorporating nanometer-sized particles. This fluid is more stable, has high thermal conductivity, high mobility, a larger heat transfer surface between particles and fluids, low pumping power compared with ordinary fluids, low particle clogging, and low volume concentrations. Ahmed et al. (2014) addressed the uncertainties of dynamic viscosity and thermal conductivity of nanofluid flow in a permeable stretching tube under the influence of a heat sink/source. They proved that the skin friction coefficient of Ag–water nanofluid is smaller compared to the TiO₂ nanofluid. The dual solutions of nanofluid flow past a moving semi-infinite flat plate are derived by Bachok et al. (2010), who found that a smaller heat transfer rate occurs in higher values of the Prandtl number. Khan and Pop (2010) explored the impact of Brownian motion and thermophoresis on a nanofluid flow in a flat surface. It is seen that Brownian motion suppresses the reduced Nusselt number and strengthens the reduced Sherwood number. The impact of Brownian motion and thermophoresis of nanofluid fluid flow between two parallel plates was recently investigated by Derakhshan et al. (2019). They proved that the Nusselt number is suppressed with enhanced thermophoretic and Brownian motion parameters. A few important works on this direction are (Hassani et al., 2011; Makinde and Aziz, 2011; Kasmani et al., 2015, 2016, 2017).

In recent years, many researchers have concerned themselves with the study of non-Newtonian materials because they have more usages in food processing, petroleum production, drawing of plastic films, metal spinning, etc. Viscoelastic fluid is one of the non-Newtonian fluids and contains viscous and elastic behaviors. Cortell (2006) discussed the MHD flow of a viscoelastic fluid past a stretching sheet with suction. He found that the viscoelastic parameter leads to an improvement of the heat transfer gradient. MHD viscoelastic boundary layer flow over a flat sheet with non-uniform heat source and radiation was analytically and numerically solved by (Abel and Mahesha, 2008). Eswaramoorthi et al. (2016) explored the effect of thermal radiation of a viscoelastic fluid over a stretching surface. They found that the velocity boundary layer thickness decays with a more enhanced viscoelastic parameter. All the above studies reported only viscoelastic fluid without nanofluid. However, in recent years, many researchers dealt with viscoelastic nanofluids because they have more industrial applications. Shit et al. (2016) examined the viscoelastic nanofluid over a stretching surface. Their result showed that the fluid temperature decays in the presence of the viscoelasticity of the nanofluid. Very recently, Hayat et al. (2018) studied the three-dimensional flow of viscoelastic nanofluid over a stretching surface with heat generation/absorption. They implemented the Cattaneo-Christov double-diffusion theory for their study. They observed that the skin friction coefficient enhances upon increasing the ratio parameter. Some useful investigations of this direction are (Ramzan and Yousaf, 2015; Ramzan et al., 2016; Seth et al., 2016). In some practical applications, such as cooling of nuclear reactors, underground disposal of radioactive waste material, and storage of foodstuffs, the heat absorption/generation effects are essential. MHD boundary layer flow of a viscoelastic nanofluid with source/sink was investigated by Goyal and Bhargava (2014) and they found that the thermal boundary layer thickens with large values for the heat source/sink parameter. Some recent discussions on heat absorption/generation can be seen in Azim et al. (2010), Eswaramoorthi et al. (2017), and Halim et al. (2017).

In nanofluids, the base fluid does not obey Newtonian fluid properties, so it becomes more justified to imagine them as viscoelastic fluids, as for example with Ethylene glycol-ZnO, Ethylene glycol-CuO and Ethylene glycol- Al_2O_3 . This type of work can be explored on two- and three-dimensional viscoelastic fluids, but less research has been done for viscoelastic nanofluids, especially three-dimensional viscoelastic nanofluids. To overcome this, we investigated the impact of passive and active controls on 3D viscoelastic nanofluid flow upon a stretching plate with heat generation and convective heating.

2. MATHEMATICAL FORMULATION

Let us consider the time-independent 3D convective flow of a heat generating viscoelastic nanofluid upon a stretched plate. Assume that the nanofluid has a single phase as well as uniform shape and size. The thermophoresis and Brownian motion effects are considered in this model. The bottom side of the plate is

heated with hot fluid of temperature T_c and makes a heat transfer coefficient h_c (see Eswaramoorthi et al., 2015, 2016). Under the above assumptions, the governing equations of the present model are given as (see Ramzan and Yousaf, 2015):

$$u_x + v_y + w_z = 0 \quad (1)$$

$$uu_x + vv_y + ww_z = \nu u_{zz} - k_1 [uu_{zzz} + wu_{zzz} - u_x u_{zz} - u_z w_{zz} - 2u_z u_{xz} - 2w_z u_{zz}] \quad (2)$$

$$uv_x + vv_y + ww_z = \nu v_{zz} - k_1 [\nu v_{zzz} + wv_{zzz} - v_x v_{zz} - v_z w_{zz} - 2v_z v_{xz} - 2w_z v_{zz}] \quad (3)$$

$$uC_x + vC_y + wC_z = D_B C_{zz} + \frac{D_T}{T_\infty} T_{zz} \quad (4)$$

$$uT_x + vT_y + wT_z = \alpha_m T_{zz} + \tau \left[D_B C_z T_z + \frac{D_T}{T_\infty} T_z^2 \right] + \frac{Q}{\rho c_p} (T - T_\infty) \quad (5)$$

where, $u, v, w, \nu, k_1, D_B, C, D_T, T, T_\infty, \alpha_m, \tau, Q, \rho,$ and c_p are the x - direction velocity, y - direction velocity, z - direction velocity, kinematic viscosity, material parameter of fluid, Brownian motion coefficient, fluid concentration, thermophoretic diffusion coefficient, temperature of the fluid, free stream temperature, thermal diffusivity, ratio of effective heat capacity of the nanoparticle material to heat capacity of the fluid, heat generation/absorption coefficient, density of the fluid and specific heat, respectively.

The corresponding boundary conditions are,

$$\begin{aligned} u(x, y, 0) &= ax, v(x, y, 0) = by, w(x, y, 0) = 0, C(x, y, 0) = C_w(x), \\ -k \frac{\partial T}{\partial z}(x, y, 0) &= h_c(T_c(x, y, 0) - T(x, y, 0)), u(x, y, \infty) = 0, v(x, y, \infty) = 0, w(x, y, \infty) = 0, \\ v_z(x, y, \infty) &= 0, C(x, y, \infty) = C_\infty, T(x, y, \infty) = T_\infty \end{aligned} \quad (6)$$

Now, we introduce the following dimensionless similarity variables,

$$\begin{aligned} u &= axf'(\eta), \quad \eta = \sqrt{\frac{a}{\nu}}z, \quad v = ayg'(\eta), \\ w &= -\sqrt{av} [f(\eta) + g(\eta)] \\ \phi(\eta) &= \frac{C - C_\infty}{C_w - C_\infty}, \quad (\text{for PC}) \quad \phi(\eta) = \frac{C - C_\infty}{C_w - C_\infty} \quad (\text{for AC}), \\ \theta(\eta) &= \frac{T - T_\infty}{T_c - T_\infty} \end{aligned} \quad (7)$$

Substituting Equation (7) in Equations (2-5), we have

$$\begin{aligned} \frac{d^3 f}{d\eta^3} - \left(\frac{df}{d\eta} \right)^2 + (f + g) \frac{d^2 f}{d\eta^2} \\ + K \left[(f + g) \frac{d^4 f}{d\eta^4} + \left(\frac{d^2 f}{d\eta^2} - \frac{d^2 g}{d\eta^2} \right) \frac{d^2 f}{d\eta^2} \right. \\ \left. - 2 \left(\frac{df}{d\eta} + \frac{dg}{d\eta} \right) \frac{d^3 f}{d\eta^3} \right] = 0 \end{aligned} \quad (8)$$

$$\begin{aligned} & \frac{d^3g}{d\eta^3} - \left(\frac{dg}{d\eta}\right)^2 + (f+g) \frac{d^2g}{d\eta^2} \\ & + K \left[(f+g) \frac{d^4g}{d\eta^4} + \left(\frac{d^2f}{d\eta^2} - \frac{d^2g}{d\eta^2}\right) \frac{d^2g}{d\eta^2} \right. \\ & \left. - 2 \left(\frac{df}{d\eta} + \frac{dg}{d\eta}\right) \frac{d^3g}{d\eta^3} \right] = 0 \end{aligned} \tag{9}$$

$$\frac{d^2\phi}{d\eta^2} + PrLe(f+g) \frac{d\phi}{d\eta} + \frac{Nt}{Nb} \frac{d^2\theta}{d\eta^2} = 0 \tag{10}$$

$$\frac{d^2\theta}{d\eta^2} + Pr(f+g) \frac{d\theta}{d\eta} + Nb \frac{d\phi}{d\eta} \frac{d\theta}{d\eta} + Nt \left(\frac{d\theta}{d\eta}\right)^2 + PrHg\theta = 0 \tag{11}$$

Boundary conditions (6) in terms of f, g, ϕ and θ become:

$$\begin{aligned} f(0) = 0, \quad g(0) = 0, \quad \frac{df(0)}{d\eta} = 1, \quad \frac{dg(0)}{d\eta} = c, \quad \frac{df(\infty)}{d\eta} = 0, \\ \frac{dg(\infty)}{d\eta} = 0, \quad \frac{d^2f(\infty)}{d\eta^2} = 0, \quad \frac{d^2g(\infty)}{d\eta^2} = 0, \\ Nb \frac{d\phi(0)}{d\eta} + Nt \frac{d\theta(0)}{d\eta} = 0, \quad \phi(\infty) = 0 \text{ (for PC)}, \\ \phi(0) = 1, \quad \phi(\infty) = 0 \text{ (for AC)} \\ \frac{d\theta(0)}{d\eta} = -Bi[1 - \theta(0)], \quad \theta(\infty) = 0 \end{aligned} \tag{12}$$

where $K = \frac{k_1 a}{\nu}$ is the viscoelastic parameter, $Pr = \frac{\nu}{\alpha_m}$ is the Prandtl number, $Nb = \frac{\tau D_B (C_w - C_\infty)}{\nu T_\infty}$ is the Brownian motion parameter, $Nt = \frac{\tau D_T (T_c - T_\infty)}{\nu T_\infty}$ is the thermophoresis parameter $Hg = \frac{Q}{a \rho c_p}$ is the heat generation/absorption parameter, $Le = \frac{\alpha_m}{De}$ is the Lewis number, $c = \frac{b}{a}$ is the stretching ratio and $Bi = \frac{h_c \sqrt{a}}{k}$ is the Biot number.

The skin friction coefficients and Nusselt number are defined as follows:

$$\begin{aligned} \tau_{wx} &= \nu u_z + k_1 [uu_{xz} + \nu u_{yz} + wu_{zz} + u_z u_x + v_z v_x + 2w_z w_x \\ & \quad - w_z u_z]_{z=0} \\ \tau_{wy} &= \nu v_z + k_1 [uv_{xz} + \nu v_{yz} + wv_{zz} + u_z u_y + v_z v_y + 2w_z w_y \\ & \quad - w_z v_z]_{z=0} \\ Nu &= - \frac{xk_T \left[\frac{\partial T}{\partial z} \right]_{z=0}}{k_T (T_w - T_\infty)} \end{aligned}$$

Then, the dimensionless form of the skin friction coefficients (C_{fx} & C_{fy}) and Nusselt number (Nu) are defined as:

$$\begin{aligned} C_{fx} \sqrt{Re} &= \left[\frac{d^2f}{d\eta^2} + K \left\{ 2 \frac{df}{d\eta} \frac{d^2f}{d\eta^2} - (f+g) \frac{d^3f}{d\eta^3} + \left(\frac{df}{d\eta} + \frac{dg}{d\eta}\right) \frac{d^2f}{d\eta^2} \right\} \right]_{\eta=0} \\ C_{fy} \sqrt{Re} &= \left[\frac{d^2g}{d\eta^2} + K \left\{ 2 \frac{dg}{d\eta} \frac{d^2g}{d\eta^2} - (f+g) \frac{d^3g}{d\eta^3} + \left(\frac{df}{d\eta} + \frac{dg}{d\eta}\right) \frac{d^2g}{d\eta^2} \right\} \right]_{\eta=0} \\ Nu/\sqrt{Re} &= - \left[\frac{d\theta}{d\eta} \right]_{\eta=0} \end{aligned}$$

3. HAM SOLUTIONS

We define the initial assumptions of HAM as $f^0(\eta) = 1 - Exp(-\eta)$, $g^0(\eta) = c(1 - Exp(-\eta))$, $\phi^0(\eta) = -\frac{NBiExp(-\eta)}{Nb(1+Bi)}$ (for PC), $\phi^0(\eta) = Exp(-\eta)$ (for AC) and $\theta^0(\eta) = \frac{BiExp(-\eta)}{1+Bi}$ and the linear operators are $L_f = \frac{d^3f}{d\eta^3} - \frac{df}{d\eta}$, $L_g = \frac{d^3g}{d\eta^3} - \frac{dg}{d\eta}$, $L_\phi = \frac{d^2\phi}{d\eta^2} - \phi$ and $L_\theta = \frac{d^2\theta}{d\eta^2} - \theta$ with $L^f [E_1 + E_2Exp(\eta) + E_3Exp(-\eta)]$, $L^g [E_4 + E_5Exp(\eta) + E_6Exp(-\eta)]$, $L^\phi [E_7Exp(\eta) + E_8Exp(-\eta)]$ and $L^\theta [E_9Exp(\eta) + E_{10}Exp(-\eta)]$, where $E_j(j = 1 - 10)$ are constants. After simplifying the m^{th} order HAM equations, we get the following:

$$\begin{aligned} f^m(\eta) &= f^{m+}(\eta) + E_1 + E_2Exp(\eta) + E_3Exp(-\eta) \\ g^m(\eta) &= g^{m+}(\eta) + E_4 + E_5Exp(\eta) + E_6Exp(-\eta) \\ \phi^m(\eta) &= \phi^{m+}(\eta) + E_7Exp(\eta) + E_8Exp(-\eta) \\ \theta^m(\eta) &= \theta^{m+}(\eta) + E_9Exp(\eta) + E_{10}Exp(-\eta) \end{aligned}$$

where $f^{m+}(\eta), g^{m+}(\eta), \phi^{m+}(\eta)$ and $\theta^{m+}(\eta)$ are the particular solutions and these solutions have the auxiliary parameters h_f, h_g, h_ϕ and h_θ . These parameters are important in the convergence of the HAM solutions. The range values are $-2.0 \leq h_f, h_g \leq -0.2$, $-1.7 \leq h_\phi \leq 0.1$, (for PC), $-1.4 \leq h_\phi \leq -0.2$ (for AC) and $-1.5 \leq h_\theta \leq 0.1$, see **Figure 1**. We found that the h value for the whole region of η is -1.

Table 1 represents the different order of $-f''(0)$, $-g''(0)$, $\phi'(0)$ and $-\theta'(0)$. It is clear that the 10th order is adequate for both velocity profiles and the 25th order is needed for both nanoparticle volume fraction and temperature profiles. **Table 2** presents the comparison of $-f''(0)$ and $-g''(0)$ for various values of c (Qayyum et al., 2014) and found that our results are in excellent agreement.

4. CORRELATION ANALYSIS

For the design of the thermal system and to analyze their performance, the correlation equations are essential. Linear regression analysis is used to derive the correlation equations from the obtained numerical values. The correlation equations of the skin friction coefficients and Nusselt number for both controls are given by:

$$\begin{aligned} C_{fx} \sqrt{Re} &= -0.713767 - 6.6843K - 0.616636c \\ C_{fy} \sqrt{Re} &= 0.439078 - 2.827825K - 1.932749c \\ Nu/\sqrt{Re} &= 0.289679 - 0.137205K + 0.034461c - 0.142392Hg \\ & \quad - 0.003866Nt - 0.000646Nb \text{ (for PC)} \\ Nu/\sqrt{Re} &= 0.279397 - 0.119256K + 0.024824c - 0.198675Hg \\ & \quad - 0.01164Nt - 0.053518Nb \text{ (for AC)} \end{aligned}$$

This equation is valid for $0 \leq K \leq 0.3$, $0 \leq c \leq 1$, $-0.3 \leq Hg \leq 0.3$, $0.2 \leq Nt \leq 1.2$ and $0.4 \leq Nb \leq 1.2$ with a maximum error of 0.05.

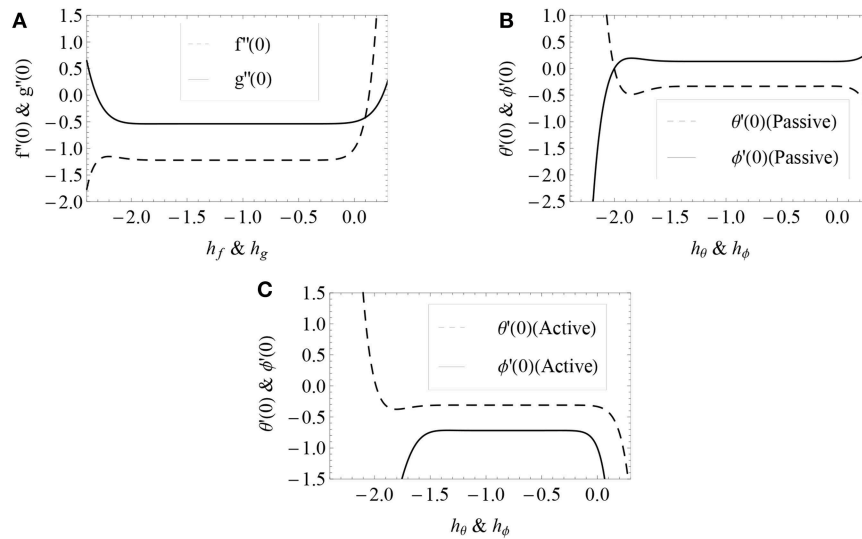


FIGURE 1 | h curves of $f''(0)$ & $g''(0)$ (A) and $\theta'(0)$ & $\phi'(0)$ for PC (B) and AC (C) with $K = 0.1$, $c = 0.5$, $Nb = 0.5$, $Nt = 0.2$, $Hg = -0.3$ and $Bi = 0.5$.

TABLE 1 | Order of approximation.

Order	$-f''(0)$	$-g''(0)$	Passive control		Active control	
			$-\theta'(0)$	$\phi'(0)$	$-\theta'(0)$	$\phi'(0)$
1	1.19167	0.529167	0.331111	0.132444	0.310123	-0.733333
5	1.22149	0.538066	0.334025	0.133610	0.309450	-0.719148
10	1.22155	0.538076	0.334214	0.133686	0.309639	-0.719172
15	1.22155	0.538076	0.334230	0.133692	0.309645	-0.719217
20	1.22155	0.538076	0.334228	0.133691	0.309643	-0.719269
25	1.22155	0.538076	0.334227	0.133691	0.309642	-0.719269
30	1.22155	0.538076	0.334227	0.133691	0.309642	-0.719269
35	1.22155	0.538076	0.334227	0.133691	0.309642	-0.719269
40	1.22155	0.538076	0.334227	0.133691	0.309642	-0.719269

TABLE 2 | Comparison of $-f''(0)$ and $-g''(0)$ for different values of c with (Qayyum et al., 2014).

c	$-f''(0)$		$-g''(0)$	
	Present study	Qayyum et al. (2014)	Present study	Qayyum et al. (2014)
0.0	1.00000	1.000000	0.00000	0.000000
0.1	1.02026	1.020259	0.06685	0.066847
0.2	1.03950	1.039495	0.14874	0.148736
0.3	1.05795	1.057954	0.24336	0.243359
0.4	1.07579	1.075788	0.34921	0.349208
0.5	1.09309	1.093095	0.46521	0.465204
0.6	1.10995	1.109946	0.59053	0.590528
0.7	1.12640	1.126397	0.72453	0.724531
0.8	1.14249	1.142488	0.86668	0.866682
0.9	1.15825	1.158253	1.01654	1.016538
1.0	1.17371	1.173720	1.17371	1.173720

5. RESULTS AND DISCUSSION

The impacts of pertinent parameters on x - direction velocity profile ($f'(\eta)$), y - direction velocity profile ($g'(\eta)$), nanoparticle volume fraction ($\phi(\eta)$), temperature profile ($\theta(\eta)$) and local Nusselt number (Nu/\sqrt{Re}) with fixed value of Prandtl number ($Pr = 1.2$) and Lewis number ($Le = 1$) are delineated in this section. **Figures 2A,B** portray the impact of viscoelastic parameter (K) on ($f'(\eta)$) and ($g'(\eta)$). In general, viscoelasticity generates tensile stress that opposes the fluid motion, and hence both velocities reduce when the values of K are enhanced. The consequences of thermophoresis parameter (Nt) and Biot number (Bi) on $\phi(\eta)$ for both controls are plotted in **Figures 3A–D**, and it was found that $\phi(\eta)$ is an enhancing function of both Nt and Bi for both controls. Physically, Nt creates a thermal conductivity of the nanoparticles. Larger thermal conductivity reveals more concentration between the nanoparticles. So, increasing the values of Nt would enrich the

nanoparticle volume fraction boundary thickness. In addition, nanoparticle volume fraction is an increasing function of the Biot number. The nanoparticle volume fraction depends on the fluid temperature. A higher Biot number causes higher fluid temperature and this causes the nanoparticle volume fraction to be enhanced. It can be seen in **Figures 4A,B** that the nanoparticle volume fraction increased along with the rising heat absorption/generation parameter (Hg) and it dropped when the values of the Brownian motion parameter (Nb) increased. This is an important result for thermal engineering applications. Physically, larger values of Nb give more kinetic energy, and this energy increases the collision between the nanoparticles. This causes the reduction of nanoparticle volume fraction layer. The impacts of Hg and Bi on $\theta(\eta)$ profile for both controls are illustrated in **Figures 5A–D**. The positive values of Hg generate

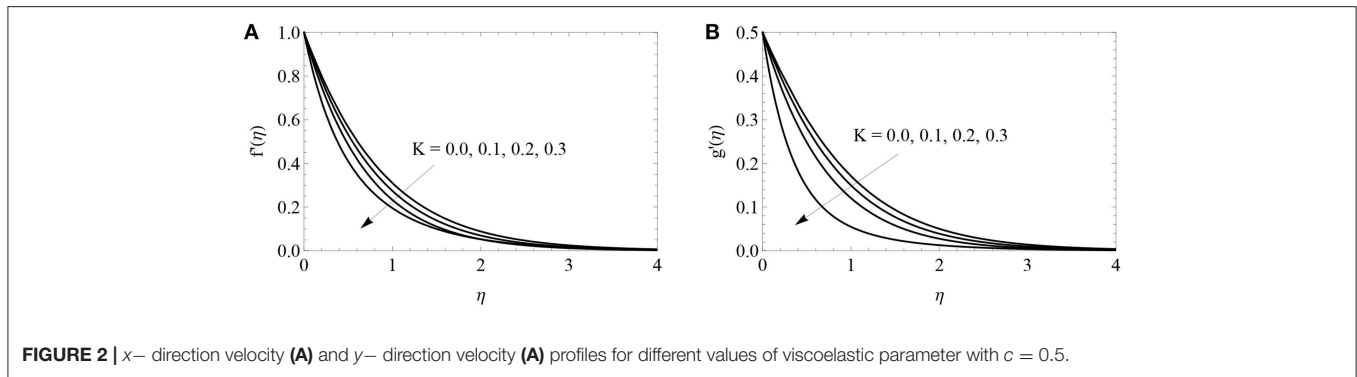


FIGURE 2 | x– direction velocity (A) and y– direction velocity (A) profiles for different values of viscoelastic parameter with $c = 0.5$.

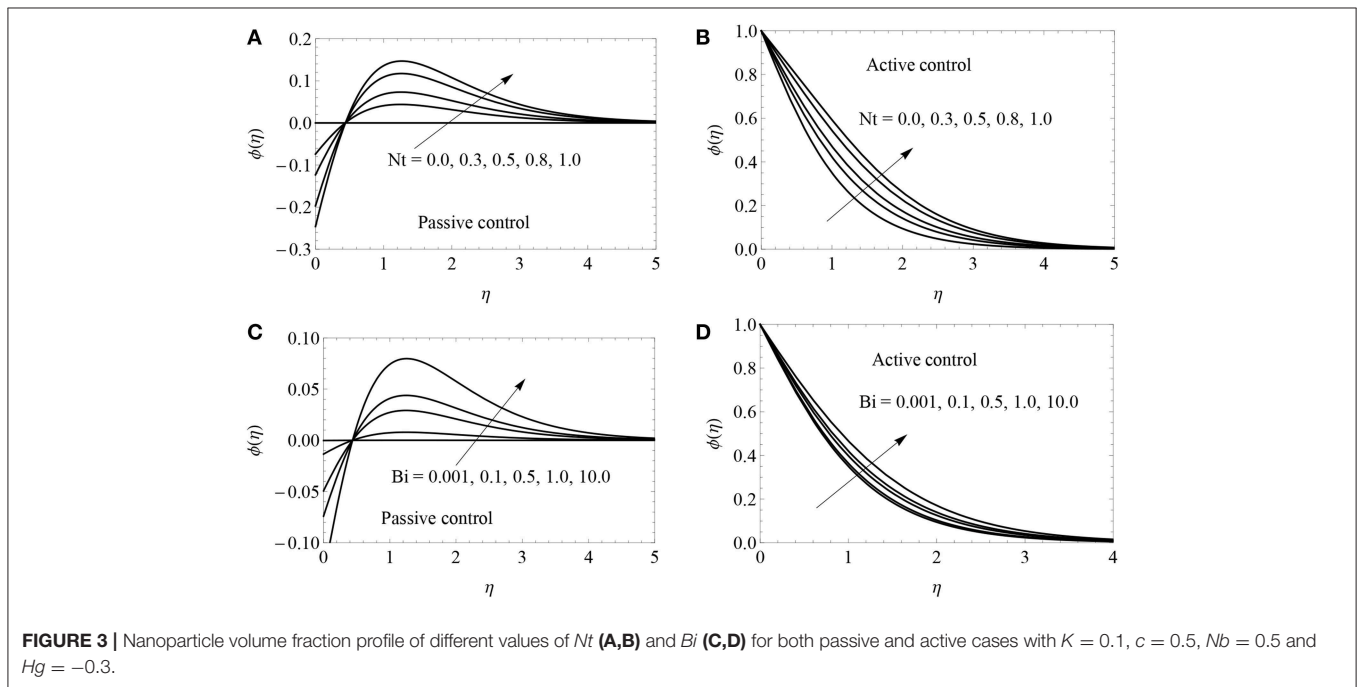


FIGURE 3 | Nanoparticle volume fraction profile of different values of Nt (A,B) and Bi (C,D) for both passive and active cases with $K = 0.1, c = 0.5, Nb = 0.5$ and $Hg = -0.3$.

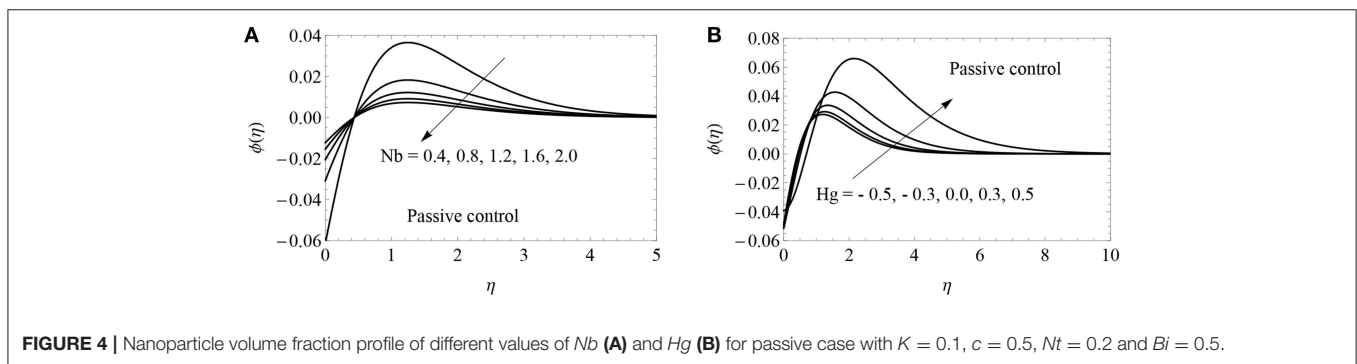
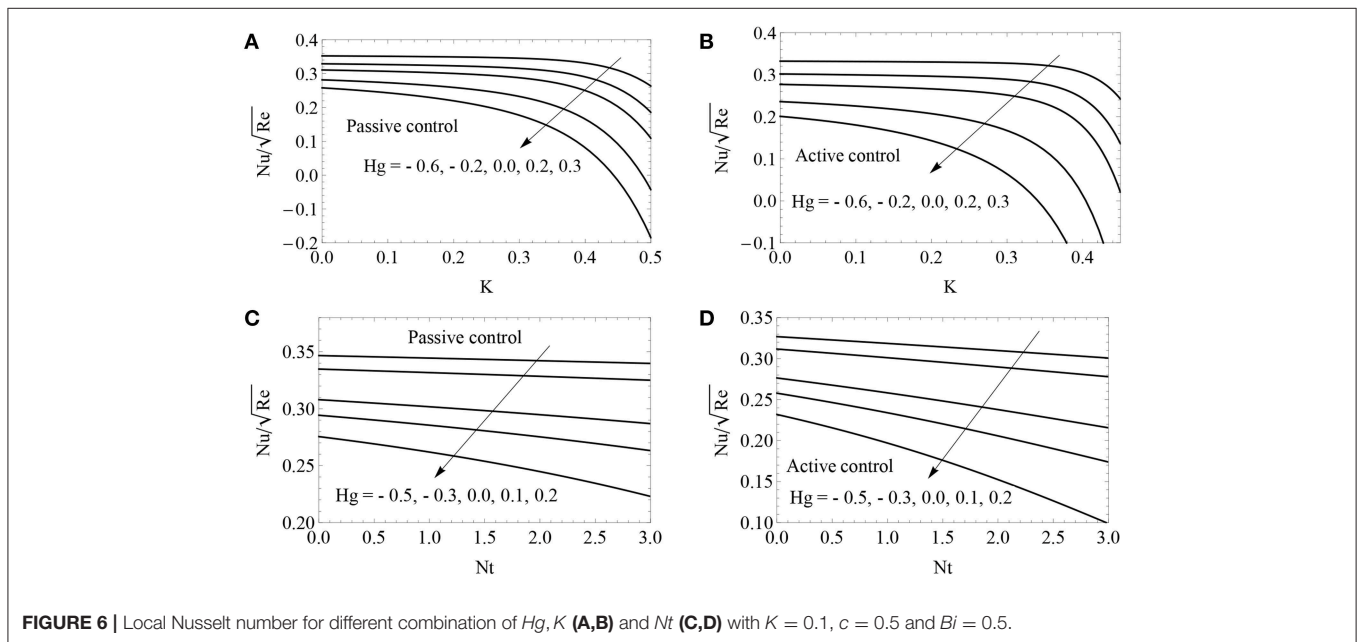
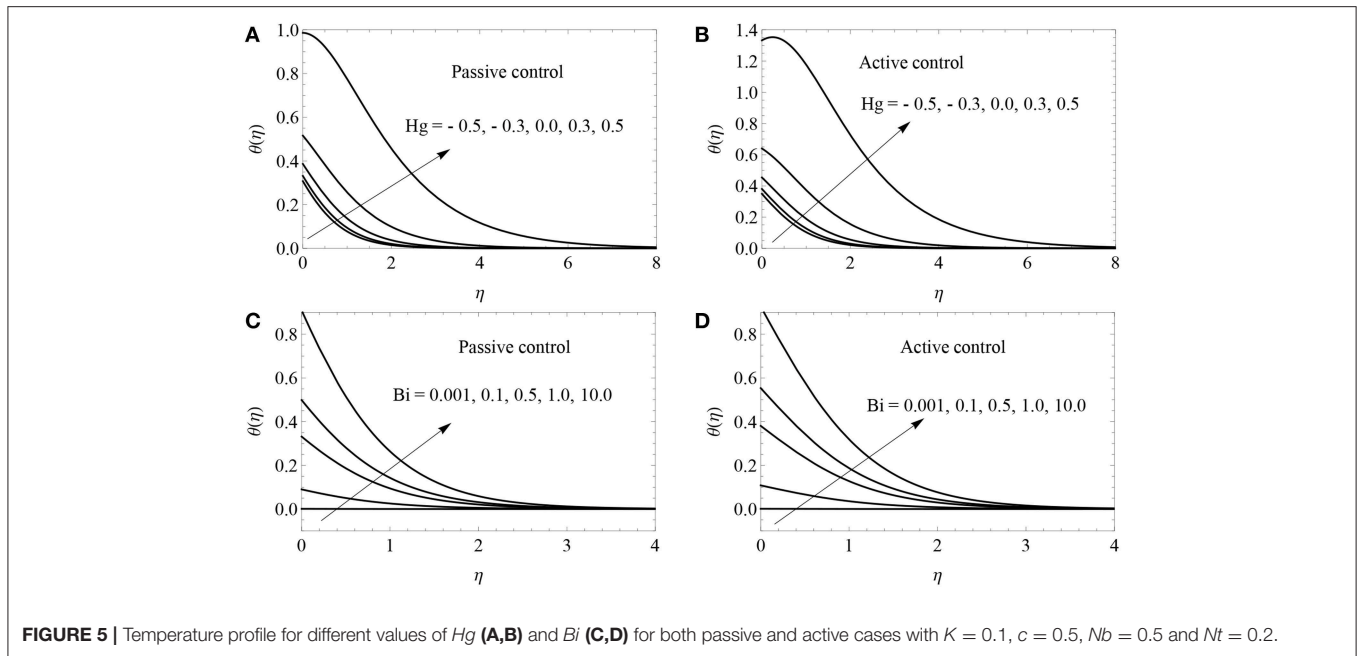


FIGURE 4 | Nanoparticle volume fraction profile of different values of Nb (A) and Hg (B) for passive case with $K = 0.1, c = 0.5, Nt = 0.2$ and $Bi = 0.5$.

heat energy inside the boundary and this causes fluid temperature to increase. On the contrary, the negative values of Hg absorb heat energy inside the boundary and this causes a reduction of the fluid temperature. Physically, the large Biot number increases the heat transfer coefficient, and this creates a higher surface

temperature. So, a larger Biot number escalates the thickness of the thermal boundary layer. This result is used to enhance heat transfer characteristics in the petroleum industry, thermal energy storage and heat exchangers. The changes of the local Nusselt number for various combinations of Hg, K and Nt are illustrated



in Figures 6A–D for both controls. These figures shows that the heat transfer gradient is reduced when the values of Hg , K and Nt are high.

6. CONCLUSIONS

In this work, we address the impact of passive control and active control on 3D viscoelastic nanofluid flow upon a stretching membrane with heat absorption/generation and

convective heating. The system of appearing non-linear PDEs is converted into a couple of ODE's by using suitable similarity transformations. Convergent series solutions are obtained using the homotopy analysis method (HAM). The following findings are observed in our study.

- Both x - direction and y - direction velocities are weakened with increasing K values.
- The nanoparticle volume fraction is strengthened when the values of Nt and Bi are high for both controls.

- The fluid temperature improves when the values of Hg and Bi increase for both controls.
- The heat transfer gradient drops when the values of Hg , K and Nt rise for both controls.

REFERENCES

- Abel, M. S., and Mahesha, N. (2008). Heat transfer in MHD viscoelastic fluid flow over a stretching sheet with variable thermal conductivity, non-uniform heat source and radiation. *Appl. Math. Model.* 32, 1965–1983. doi: 10.1016/j.apm.2007.06.038
- Ahmed, S. E., Hussein, A. K., Mohammed, H. A., and Sivasankaran, S. (2014). Boundary layer flow and heat transfer due to permeable stretching tube in the presence of heat source/sink utilizing nanofluids. *Appl. Math. Comp.* 238, 149–162. doi: 10.1016/j.amc.2014.03.106
- Azim, M. A., Mamun, A. A., and Rahman, M. M. (2010). Viscous Joule heating MHD-conjugate heat transfer for a vertical flat plate in the presence of heat generation. *Int. Commu. Heat Mass Transf.* 37, 666–674. doi: 10.1016/j.icheatmasstransfer.2010.02.002
- Bachok, N., Ishak, A., and Pop, I. (2010). Boundary-layer flow of nanofluids over a moving surface in a flowing fluid. *Int. J. Ther. Sci.* 49, 1663–1668. doi: 10.1016/j.ijthermalsci.2010.01.026
- Cortell, R. (2006). Effects of viscous dissipation and work done by deformation on the MHD flow and heat transfer of a viscoelastic fluid over a stretching sheet. *Physica Letters A.* 357, 298–305. doi: 10.1016/j.physleta.2006.04.051
- Derakhshan, R., Ahmadreza Shojaei, Hosseinzadeh, K. H., Nimafar, M., and Ganji, D. D. (2019). Hydrothermal analysis of magneto hydrodynamic nanofluid flow between two parallel by AGM. *Case Studies Ther. Engin.* 14, 100439. doi: 10.1016/j.csite.2019.100439
- Eswaramoorthi, S., Bhuvanewari, M., Sivasankaran, S., and Rajan, S. (2015). Effect of radiation on MHD convective flow and heat transfer of a viscoelastic fluid over a stretching surface. *Procedia Eng.* 127, 916–923. doi: 10.1016/j.proeng.2015.11.364
- Eswaramoorthi, S., Bhuvanewari, M., Sivasankaran, S., and Rajan, S. (2016). Soret and Dufour effects on viscoelastic boundary layer flow, heat and mass transfer in a stretching surface with convective boundary condition in the presence of radiation and chemical reaction. *Scientia Iranica Transactions B: Mech. Engin.* 23, 2575–2586. doi: 10.24200/sci.2016.3967
- Eswaramoorthi, S., Bhuvanewari, M., Sivasankaran, S., and Rajan, S. (2017). Effect of partial slip and chemical reaction on convection of a viscoelastic fluid over a stretching surface with Cattaneo-Christov heat flux model. *IOP Conf. Ser. Mater. Sci. Eng.* 263, 1–8. doi: 10.1088/1757-899X/263/6/062009
- Goyal, M., and Bhargava, R. (2014). Boundary layer flow and heat transfer of viscoelastic nanofluids past a stretching sheet with partial slip conditions. *Appl. Nanosci.* 4, 761–767. doi: 10.1007/s13204-013-0254-5
- Halim, N. A., Sivasankaran, S., and Noor, N. F. M. (2017). Active and passive controls of the Williamson stagnation nanofluid flow over a stretching/shrinking surface. *Neural Comput. Appl.* 28, 1023–1033. doi: 10.1007/s00521-016-2380-y
- Hassani, M., Mohammad Tabar, M., Nemati, H., Domairry, G., and Noori, F. (2011). An analytical solution for boundary layer flow of a nanofluid past a stretching sheet. *Int. J. Ther. Sci.* 50, 2256–2263. doi: 10.1016/j.ijthermalsci.2011.05.015

AUTHOR CONTRIBUTIONS

All authors listed have made a substantial, direct and intellectual contribution to the work, and approved it for publication.

- Hayat, T., Qayyum, S., Shehzad, S. A., and Alsaedi, A. (2018). Cattaneo-Christov double-diffusion theory for three-dimensional flow of viscoelastic nanofluid with the effect of heat generation/absorption. *Res. Phys.* 8, 489–495. doi: 10.1016/j.rinp.2017.12.060
- Kasmani, R. M., Sivasankaran, S., Bhuvanewari, M., and Hussein, A. K. (2017). Analytical and numerical study on convection of nanofluid past a moving wedge with Soret and Dufour effects. *Int. J. Numer. Methods Heat Fluid Flow.* 27, 2333–2354. doi: 10.1108/HFF-07-2016-0277
- Kasmani, R. M., Sivasankaran, S., Bhuvanewari, M., and Siri, Z. (2015). Effect of thermal radiation and suction on convective heat transfer of nanofluid along a wedge in the presence of heat generation/absorption. *AIP Conf. Proc.* 1682, 020008-1–020008-7. doi: 10.1063/1.4932417
- Kasmani, R. M., Sivasankaran, S., Bhuvanewari, M., and Siri, Z. (2016). Effect of chemical reaction on convective heat transfer of boundary layer flow in nanofluid over a wedge with heat generation/absorption and suction. *J. Appl. Fluid Mech.* 3, 379–388. doi: 10.18869/acadpub.jafm.68.224.24151
- Khan, W. A., and Pop, I. (2010). Boundary-layer flow of a nanofluid past a stretching sheet. *Int. J. Heat Mass Transf.* 53, 2477–2483. doi: 10.1016/j.ijheatmasstransfer.2010.01.032
- Makinde, O. D., and Aziz, A. (2011). Boundary layer flow of a nanofluid past a stretching sheet with a convective boundary condition. *Int. J. Ther. Sci.* 50, 1326–1332. doi: 10.1016/j.ijthermalsci.2011.02.019
- Qayyum, A., Hayat, T., Alhuthali, M. S., and Malaikah, H. M. (2014). Newtonian heating effects in three-dimensional flow of viscoelastic fluid. *ICHin. Phys. B.* 23, 054703. doi: 10.1088/1674-1056/23/5/054703
- Ramzan, M., and Yousaf, F. (2015). Boundary layer flow of three-dimensional viscoelastic nanofluid past a bi-directional stretching sheet with Newtonian heating. *AIP Advances* 5, 057132-1-057132-15. doi: 10.1063/1.4921312
- Ramzan, M., Yousaf, F., Farooq, M., and Chung, J. D. (2016). Mixed convective viscoelastic nanofluid flow past a porous media with Soret-Dufour effects. *Commu. Theoret. Phys.* 66, 133–142. doi: 10.1088/0253-6102/66/1/133.
- Seth, G. S., Mishra, M. K., and Chamkha, A. J. (2016). Hydromagnetic convective flow of viscoelastic nanofluid with convective boundary condition over an inclined stretching sheet. *J. Nanofluids.* 5, 511–521. doi: 10.1166/jon.2016.1249
- Shit, G. C., Haldar, R., and Ghosh, S. K. (2016). Convective heat transfer and MHD viscoelastic nanofluid flow induced by a stretching sheet. *Int. J. Appl. Comput. Math.* 2, 593–608. doi: 10.1007/s40819-015-0080-4

Conflict of Interest Statement: The authors declare that the research was conducted in the absence of any commercial or financial relationships that could be construed as a potential conflict of interest.

Copyright © 2019 Eswaramoorthi and Bhuvanewari. This is an open-access article distributed under the terms of the Creative Commons Attribution License (CC BY). The use, distribution or reproduction in other forums is permitted, provided the original author(s) and the copyright owner(s) are credited and that the original publication in this journal is cited, in accordance with accepted academic practice. No use, distribution or reproduction is permitted which does not comply with these terms.